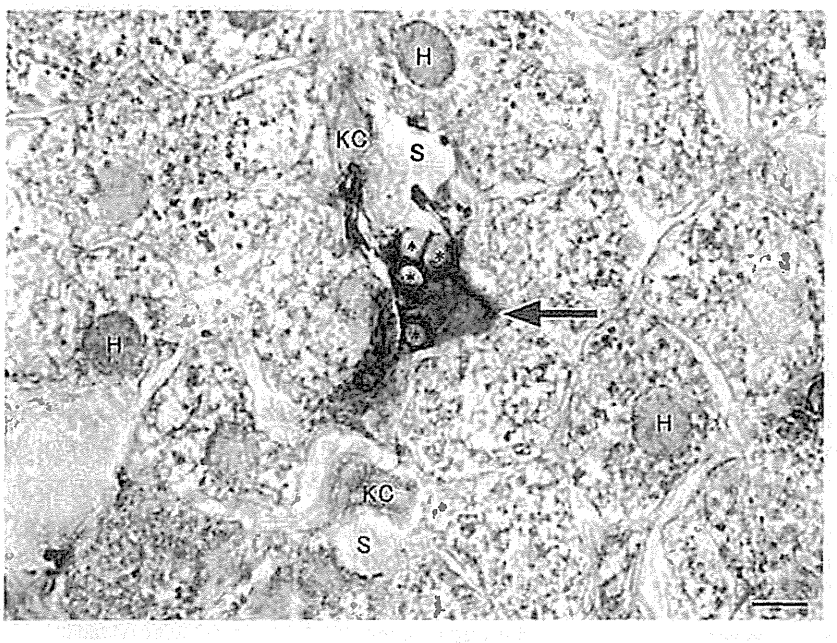

図1　肝小葉内の星細胞

抗heat shock protein 47 (HSP47) 抗体による免疫組織染色像．HSP47はコラーゲン産生細胞に発現し，肝小葉内では星細胞（矢印）が特異的に有する．星細胞は類洞 (S) の周囲に位置し，多数の脂肪滴（＊）を持つ．

H：肝細胞，KC：Kupffer細胞，scale bar：5 μm

の産生が著増し，さらに，組織メタロプロテアーゼ阻害物 (tissue inhibitor of matrix metalloproteinases；TIMP) を産生することでECMの分解が阻害されて組織局所に線維成分が蓄積する．また，トランスフォーミング増殖因子β1 (transforming growth factor β1；TGFβ1) をはじめとする炎症性サイトカインやケモカインを分泌して，マクロファージやT細胞などの免疫担当細胞を誘導し，炎症を進展させる．TGFβ1などはautocrine的にも作用し，星細胞の持続的活性化を引き起こす．

活性化星細胞ではビタミンAが失われていく．ビタミンAを外来性に投与することによって，星細胞の活性化が抑制され，実験的肝線維症の進展が阻害されることが知られている．また，活性化星細胞では，平滑筋αアクチン (α-smooth muscle actin) を主体とするストレスファイバーが形成され，細胞の収縮性が増大することによって組織の硬変化に拍車をかける．

従来，肝線維化の責任細胞は活性化星細胞であると考えられてきた．しかし近年，肝線維化巣の筋線維芽細胞には複数の由来があることが議論されており，特にGlisson鞘の線維芽細胞が注目されている[7]．肝線維化の責任細胞の主体は病態によって変化することが示唆されており，肝線維化の治療戦略を構築する上でもさらなる研究の進展が待たれるところである．

文 献

1) 和氣健二郎：解剖誌 72：407, 1997.
2) Wake K：Int Rev Cytol 66：303, 1980.
3) Hepatic stellate cell nomenclature.：Hepatology 23：193, 1996.
4) Hellerbrand C：Pflugers Arch 465：775, 2013.
5) Nakatani K, et al：Lab Invest 84：91, 2004.
6) 元山宏行，他：医学のあゆみ 240：699, 2012.
7) Brenner DA, et al：Fibrogenesis Tissue Repair 5：S17, 2012.

回 答

大阪市立大学 大学院医学研究科
機能細胞形態学（解剖学第一）
1) 准教授　2) 教授
1) 仲谷和記　2) 池田一雄

Hepatology Research

Hepatology Research 2013 doi: 10.1111/hepr.12165

Original Article

Effects of oral intake of hydrogen water on liver fibrogenesis in mice

Yukinori Koyama,[1] Kojiro Taura,[1] Etsuro Hatano,[1] Kazutaka Tanabe,[1] Gen Yamamoto,[1] Kojiro Nakamura,[1] Kenya Yamanaka,[1] Koji Kitamura,[1] Masato Narita,[1] Hiromitsu Nagata,[1] Atsuko Yanagida,[1] Taku Iida,[1] Keiko Iwaisako,[1] Hikohito Fujinawa[2] and Shinji Uemoto[1]

[1]*Department of Surgery, Graduate School of Medicine, Kyoto University, Kyoto, and* [2]*Quality and Reliability Assurance Division, Sun Pharma Japan, Tokyo, Japan*

Aim: Liver fibrosis is the universal consequence of chronic liver diseases. Sustained hepatocyte injury initiates an inflammatory response, thereby activating hepatic stellate cells, the principal fibrogenic cells in the liver. Reactive oxygen species are involved in liver injury and are a promising target for treating liver fibrosis. Hydrogen water is reported to have potential as a therapeutic tool for reactive oxygen species-associated disorders. This study aimed to investigate the effects of hydrogen water on liver fibrogenesis and the mechanisms underlying these effects.

Methods: C57BL/6 mice were fed with hydrogen water or control water, and subjected to carbon tetrachloride, thioacetamide and bile duct ligation treatments to induce liver fibrosis. Hepatocytes and hepatic stellate cells were isolated from mice and cultured with or without hydrogen to test the effects of hydrogen on reactive oxygen species-induced hepatocyte injuries or hepatic stellate cell activation.

Results: Oral intake of hydrogen water significantly suppressed liver fibrogenesis in the carbon tetrachloride and thioacetamide models, but these effects were not seen in the bile duct ligation model. Treatment of isolated hepatocyte with 1 μg/mL antimycin A generated hydroxyl radicals. Culturing in the hydrogen-rich medium selectively suppressed the generation of hydroxyl radicals in hepatocytes and significantly suppressed hepatocyte death induced by antimycin A; however, it did not suppress hepatic stellate cell activation.

Conclusion: We conclude that hydrogen water protects hepatocytes from injury by scavenging hydroxyl radicals and thereby suppresses liver fibrogenesis in mice.

Key words: hydrogen, hydrogen water, hydroxyl radical, liver cirrhosis, liver fibrosis, liver injury

INTRODUCTION

LIVER FIBROSIS IS a common cause of death worldwide.[1] Advanced liver fibrosis disrupts normal liver architecture, causing hepatocellular dysfunction and portal hypertension. To date, no effective hepatic antifibrotic therapies are available.

The hepatic stellate cell (HSC) is the major fibrogenic cell type in the liver.[2] Sustained hepatocyte injuries such as those caused by hepatitis viruses and alcohol, lead to the activation of HSC and hepatocyte death, which is induced by the activation of inflammatory mediators such as transforming growth factor (TGF)-β1.[3] HSC are activated to differentiate into myofibroblast-like cells, which promote collagen deposition.

Reactive oxygen species (ROS) play an important role in hepatic fibrosis.[4] Galli *et al.* reported that the superoxide anion ($O^{\cdot}_{2^-}$) produced by xanthine and xanthine oxidase induced the proliferation of HSC.[5] On the other hand, Sandra *et al.* reported that rather than directly inducing HSC proliferation, hydrogen peroxide (H_2O_2) and $O^{\cdot}_{2^-}$ inhibited the proliferation of these cells.[6] To date, it is unclear how ROS contribute to the development of liver fibrogenesis.

Oxidative stress arises from the strong cellular oxidizing potential of ROS or free radicals. Most of the $O^{\cdot}_{2^-}$ is generated in the mitochondria by electron leakage from the electron-transport chain and the Krebs cycle.[7,8] $O^{\cdot}_{2^-}$ is also generated by metabolic oxidases, including nicotinamide adenine dinucleotide phosphate oxidase and

Correspondence: Dr Kojiro Taura, Department of Surgery, Graduate School of Medicine, Kyoto University, 54 Kawahara-cho, Shogoin, Sakyo-ku, Kyoto 606-8507 Japan. Email: ktaura@kuhp.kyoto-u.ac.jp
Received 11 December 2012; revision 5 May 2013; accepted 14 May 2013.

xanthine oxidase.[5,9] Superoxide dismutase converts $O\cdot_2^-$ into H_2O_2. Excess $O\cdot_2^-$ reduces transition metal ions, such as Fe^{3+} and $Cu,^{2+}$ and the reduced forms can react with H_2O_2 to produce hydroxyl radicals ($OH\cdot$) by the Fenton reaction. $OH\cdot$ is the strongest ROS and reacts indiscriminately with nucleic acids, lipids and proteins.[10]

Recent studies have shown that hydrogen acts as an antioxidant. A study by Ohsawa *et al.* on a model of brain ischemia–reperfusion injury revealed that hydrogen was a selective antioxidant for $OH\cdot$.[11] The beneficial effect of hydrogen was also reported recently in various models of liver injury, such as ischemia–reperfusion injury and injury induced by galactosamine lipopolysaccharide.[12] Sun *et al.* reported that i.p. injection with hydrogen-rich saline was also effective in a model of carbon tetrachloride (CCl_4)-induced liver fibrosis.[12] However, they examined the effects only in a hepatic injury model, and the pathophysiological mechanism by which hydrogen-rich saline attenuates liver fibrosis remains to be elucidated. Further, the applicability of hydrogen would be more widespread if orally ingested hydrogen water (H_2-water) could effectively suppress liver fibrogenesis.

This study aimed to investigate the effects of H_2-water on various liver injury models and the mechanisms underlying these effects.

METHODS

Animals and treatment

MALE C57BL/6 MICE were purchased from Clea Japan (Tokyo, Japan). The mice were treated with CCl_4, thioacetamide (TAA) or bile duct ligation (BDL) to induce liver fibrosis. The mice were fed with H_2-water or control water while liver fibrosis was induced. In the CCl_4 model, the 7-week-old mice were injected i.p. with 0.5 μL of CCl_4 per gram mouse weight twice a week for 6 weeks ($n = 20$ for hydrogen water and control water group).[13] Corn oil was injected as a control ($n = 3$ for each group). In the TAA model, the mice were injected i.p. with escalating dose of TAA twice a week for 6 weeks (first dose, 100 μg/g; weeks 1–2, 200 μg/g; week 3, 4300 μg/g; weeks 4–6, 400 μg/g) ($n = 6$ for each group).[14] Normal saline was injected as a control ($n = 3$ for each group). BDL was performed by surgical ligation of the common hepatic bile duct with 6-0 nylon under pentobarbital anesthesia (50 mg/kg) ($n = 6$ for each group). Sham-operated mice underwent a laparotomy without ligation of the common bile duct ($n = 3$ for each group). The animals were killed on postoperative day 21. The animal protocols were approved by the Animal Research Committee of Kyoto University, and all experiments were conducted in accordance with Guidelines for the Care and Use of Laboratory Animals promulgated by the National Institute of Health.

H_2-water and hydrogen-rich medium

Hydrogen water at the concentration of 1.24 mg/L and control water were provided in 300-mL aluminum pouches supplied by I'rom Pharmaceutical (Tokyo, Japan). The mice were provided water ad libitum through closed glass vessels (I'rom Pharmaceutical) equipped with an outlet line containing two ball bearings, which prevented the degassing of the water. The vessel was freshly refilled with H_2-water every day.

The hydrogen-rich medium was prepared according to a method described previously.[15] In brief, hydrogen gas was dissolved directly into the media by bubbling the gas into the medium.

Isolation and culture of hepatocytes

Hepatocytes were isolated from mouse livers by a previously described method.[16] The isolated hepatocytes were cultured on six-well plates coated with type 1 collagen, at a cell density of 5×10^5 cells/well, in Dulbecco's modified Eagle's medium (DMEM) supplemented with 10% fetal calf serum, 100 U/mL penicillin and 100 μg/mL streptomycin at 37°C in a humidified atmosphere of 5% CO_2 and 95% air.

Isolation and culturing of HSC

Hepatic stellate cells were isolated from mouse livers by a method described previously.[17,18] In brief, liver cells were dispersed with 0.025% PronaseE (Merck, Darmstadt, Germany) and 0.025% collagenase (Wako, Osaka, Japan). The cell suspension was centrifuged through 9.7% Nycodenz (Nycomed Pharm, Oslo, Norway) cushion. The HSC-enriched band was transferred into DMEM, supplemented with 10% fetal bovine serum and antibiotics. The isolated HSC was incubated in a CO_2 incubator at 37°C. The purity of HSC was consistently more than 98% as judged by presence of lipid droplets and autofluorescence.

To analyze whether the hydrogen-rich medium suppresses HSC activation, the isolated HSC were cultured in hydrogen-rich medium for 5 days, during which the medium was changed every day.

ROS induction with antimycin A and detection of ROS

To examine the effects of ROS induction for hepatocytes, the medium was replaced with serum-free

DMEM 6 h after plating. Twelve hours later, 1 μg/mL antimycin A (AMA; Sigma-Aldrich, St Louis, MO, USA) was added, and the cells were incubated for 1 h. Then, the cells were stained with bisbenzimide H33342 fluorochrome dihydrochloride dimethylsulfoxide solution (Hoechst 33342; Nacalai Tesque, Kyoto, Japan) and propidium iodide (PI; Calbiochem, San Diego, CA, USA) and examined under a fluorescent microscope. Five non-overlapping fields at ×200 magnifications were photographed at random. PI positive cells were considered as dead cells, and the PI positive ratio was calculated as the percentage of PI positive cells among the Hoechst 33342 positive cells. For the detection of $OH\cdot$, O_{2}^{-} and H_2O_2, the cells were incubated with MitoSOX, 2′,7′-dichlorodihydrofluorescein (CM-H_2DCFDA) and hydroxyphenyl fluorescein (HPF; Nikken Seil, Shizuoka Japan), respectively.[19,20]

To examine whether HSC activation is accelerated by ROS, the medium was replaced with serum-free DMEM 24 h after plating. Twenty-four hours later, 1 μg/mL AMA (Sigma-Aldrich) was added, and the cells were incubated for 1 h. The cells were observed with a BIOREVO BZ-9000 digital microscope (Keyence, Osaka, Japan) at ×200 magnifications.

Immunohistochemistry

The specimens were fixed in 4% paraformaldehyde and embedded in optimal cutting temperature compound. Slices of the specimens at 4-μm thickness were obtained, and the antigen was retrieved by incubation in citric acid buffer at 90°C for 20 min. After being blocked, the sections were incubated with primary antibody-recognizing α-smooth muscle actin (α-SMA; no. ab5694; Abcam, Cambridge, UK) at 1:200 dilution overnight at 4°C and then incubated with antibody-recognizing rabbit immunoglobulin (Ig)G labeled by Alexa594 (Invitrogen, Tokyo, Japan) at room temperature for 1 h.

For the detection of 3-nitrotyrosine, the sections were incubated for 1 h in a working solution of mouse IgG blocking reagent from the MOM Immunodetection kit (Vector, Burlingame, CA, USA), and then incubated sequentially with 3-nitrotyrosine-recognizing primary antibody (Mab5404; Merck) at 1:100 dilution overnight at 4°C, MOM biotinylated antimouse IgG reagent for 10 min and VECTASTAIN ABC reagent for 5 min. The sections were examined after incubation with Liquid DAB Substrate Chromogen System (Dako, Glostrup, Denmark) for 3 min.

Liver histology

Formalin-fixed, paraffin-embedded specimens were sliced at 4-μm thickness and mounted on silanized glass slides. The slides were stained with Sirius red.[21] Images of five non-overlapping fields were randomly selected and captured at ×200 magnifications. Sirius red staining was quantified by image analysis with National Institutes of Health image (Image J).

Hydroxyproline contents

Liver tissues were homogenized in ice-cold distilled water (1 mL). One hundred and twenty-five microliters of 50% tricarboxylic acid (TCA) was added and the homogenates were further incubated on ice for 30 min. The precipitated pellets were hydrolyzed for 24 h at 110°C in 6 N HCL. Samples were filtered and neutralized with 10 N NaOH. Hydrolysates were then oxidized with chloramine-T (Sigma, St Louis, MO, USA) for 25 min at room temperature. The reaction mixture was incubated in Ehrich's perchloric acid solution at 65°C for 20 min, and then cooled at room temperature. Sample absorbance was measured at 560 nm. Purified hydroxyproline (Sigma) was used to set a standard. Hydroxyproline content was expressed as nanograms of hydroxyproline per milligram of liver.

ROS analysis for the liver specimens

Accumulation of ROS in the liver was assessed by staining freshly frozen liver sections with HPF. In brief, the freshly frozen liver specimens were sliced at 4-μm thickness and were incubated with HPF diluted at 1:200 for 15 min at 37°C.

The malondialdehyde (MDA) level was determined according to the thiobarbituric acid method using an NWLSS Malondialdehyde Assay Kit (Northwest Life Science Specialties, Vancouver, WA, USA).

Glutathione (GSH) level was determined with a GSH quantification assay kit (Dojindo, Tokyo, Japan).

Biochemical measurements were carried out at room temperature using a spectrophotometer (Molecular Devices, Tokyo, Japan).

Western blotting

The protocol for western blotting was described previously.[16] The primary antibodies and dilutions were as follows: anti-α-SMA antibody (no. ab5694; Abcam) at 1:1000; and anti-α-tubulin antibody (no. CP06; Calbiochem) at 1:1000.

Quantitative reverse transcription polymerase chain reaction analysis

Total RNA was extracted from the liver sample or isolated HSC by RNeasy Mini Kit with on-column DNA digestion (Qiagen, Tokyo, Japan). Total RNA was reverse transcribed to complementary DNA by using the Omniscript RT Kit (Qiagen, Valencia, CA, USA). Quantitative real-time reverse transcription polymerase chain reaction (RT–PCR) was performed using SYBR Green Master reaction mix on a LightCycler 480 II (Roche Diagnostics, Basel, Switzerland). The relative abundance of the target genes was obtained by calculating against a standard curve and normalized to glyceraldehyde 3-phosphate dehydrogenase (GAPDH) for liver samples, and to 18S ribosomal RNA for HSC samples, as the internal control. The primer sequences used were: Col-1α1, forward 5′-GCT CCT CTT AGG GGC CAC T-3′, reverse 5′-CCA CGT CTC ACC ATT GGG G-3′; α-SMA, forward 5′-GTC CCA GAC ATC AGG GAG TAA-3′, reverse 5′-TCG GAT ACT TCA GCG TCA GGA-3′; TGF-β1, forward 5′-CCG CAA CAA CGC CAT CTA TG-3′, reverse 5′-CCC GAA TGT CTG ACG TAT TGG AAG-3′; GAPDH, forward 5′-AGG TCG GTG TGA ACG GAT TTG-3′, reverse 5′-TGT AGA CCA TGT AGT TGA GGT CA-3′; and 18 s ribosomal RNA, forward 5′-AGT CCC TGC CCT TTG TAC ACA-3′, reverse 5′-CGA TCC GAG GGC CTC ACT A-3′.

Statistical analysis

Each quantitative dataset was presented as mean ± standard error of the mean, and statistically analyzed with two-tailed Student's *t*-test followed by a post-hoc Fisher's protected least significant difference test.

RESULTS

Oral intake of H_2-water suppressed liver fibrogenesis in models of CCl_4- and TAA-induced liver injury

IN THE CCl_4 model, hepatic hydroxyproline content was significantly lower in the H_2-water group than the control water group (295.0 vs 382.6 ng/mg liver; $P < 0.05$) (Fig. 1a). Liver fibrosis, assessed by the intensity of Sirius red staining, was inhibited in the H_2-water group (Fig. 1b). Sirius red staining showed that the fibrotic area with collagen deposit was 8.163% in the control water group and 4.666% in the H_2-water group ($P < 0.0001$) (Fig. 1b). The inhibitory effect of H_2-water on liver fibrogenesis were further evaluated by RT–PCR for collagen1α1 and α-SMA. In the H_2-water group and control water group, the mRNA levels of collagen1α1 were 4.77 and 11.55 times that in the control ($P < 0.05$), while those of α-SMA were 2.15 and 3.92 times that in the control ($P < 0.05$) (Fig. 1c), respectively. Western blotting showed that the α-SMA levels in the H_2-water group and control water group was 1.64 and 2.87 times that in the control, respectively ($P < 0.01$) (Fig. 1d). H_2-water also suppressed the mRNA level of TGF-β1 (3.03 vs 1.74 times as control; $P < 0.05$) in the liver.

In the TAA model, H_2-water drinking suppressed liver fibrogenesis, as assessed by the hydroxyproline content (232.7 vs 287.1 ng/mg liver; $P < 0.05$) (Fig. 2a), Sirius red staining (2.563% vs 4.271%; $P < 0.01$) (Fig. 2b), RT–PCR for collagen1α1 (7.88 vs 59.4 times that in the control; $P < 0.01$) and α-SMA (2.24 vs 26.62 times that in the control; $P < 0.01$) (Fig. 2c), and western blotting for α-SMA (4.86 vs 9.96 times that in the control; $P < 0.01$) (Fig. 2d). H_2-water suppressed the mRNA level of TGF-β1 (3.37 vs 2.07 times in the control; $P < 0.05$) in the liver.

H_2-water oral intake suppressed generation of hydroxyl radicals in the liver

Hydroxyphenyl fluorescein staining for the detection of OH· on freshly frozen liver sections in the CCl_4 model showed a significantly smaller area of HPF staining in the H_2-water group (Fig. 3a) than in the control water group; this indicated that orally ingested H_2-water had a scavenging effect on OH· in the liver. These results demonstrated that CCl_4 injection induced the release of OH· and that H_2-water scavenged OH·. In the TAA model, HPF staining was present in a significantly smaller area in the H_2-water group (Fig. 3b).

Malondialdehyde levels in the H_2-water group were significantly lower in the CCl_4 model (3.89 vs 1.57 times that in the control) and TAA model (2.17 vs 1.41 times that in the control) (Fig. 3c). These results supports the antioxidative effect of H_2-water on OH· which generates lipid peroxidation. H_2-water did not change 3-nitrotyrosine expression (Fig. 4a,b) and GSH level (Fig. 4c).

Inhibition of CCl_4- or TAA-induced liver fibrosis by H_2-water was associated with less hepatocyte damage

The H_2-water group showed significantly lower transaminase levels in CCl_4 model at day 1 after CCl_4 injection (aspartate aminotransferase [AST], 2532 ± 697 [H_2-water] vs 5133 ± 908 IU/L [control water]; alanine aminotransferase [ALT], 3441 ± 790 [H_2-water] vs 6756 ± 1166 IU/L [control water]) and in TAA model at day 1 after TAA injection (AST, 1066 ± 460 [H_2-water] vs 2906 ± 834 IU/L [control water]; ALT, 1197 ± 442 [H_2-water] vs 4018 ± 997 IU/L [control water]).

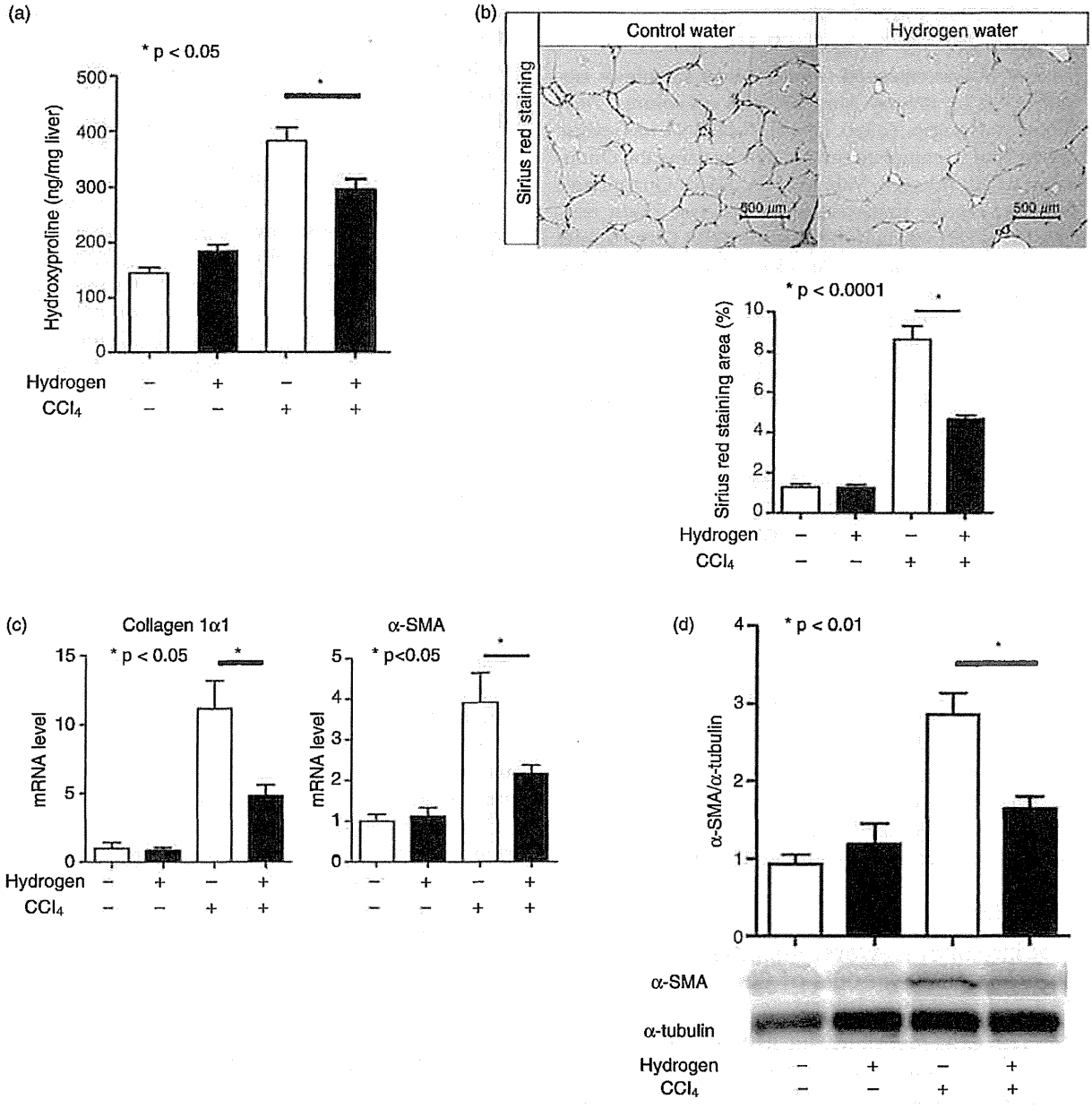

Figure 1 Oral intake of H_2-water suppresses carbon tetrachloride (CCl_4)-induced liver fibrogenesis in mice. C57BL/6 mice were subjected to repeated injections with CCl_4 and fed with hydrogen water (H_2-water) or control water. The hepatic hydroxyproline content was significantly lower in the H_2-water group than in the control water group (295.0 vs 382.6 ng/mg liver; $P < 0.05$) (a). Liver fibrosis, which was assessed by Sirius red staining, was inhibited in the H_2-water group. Fibrotic area with collagen deposit was 8.163% in the control water group and 4.666% in the H_2-water group ($P < 0.0001$), as determined by Sirius red staining (b). The mRNA levels of collagen1α1 in the H_2-water group and the control water group was 4.77 and 11.15 times that in the control, respectively ($P < 0.05$). The mRNA level of α-smooth muscle actin (α-SMA) was 2.15 times that in the controls in the H_2-water group and 3.92 times that in the controls in the control water group ($P < 0.05$) (c). Western blotting for α-SMA in the H_2-water group and the control water group were 1.64 and 2.87 times that in the control, respectively ($P < 0.01$) (d).

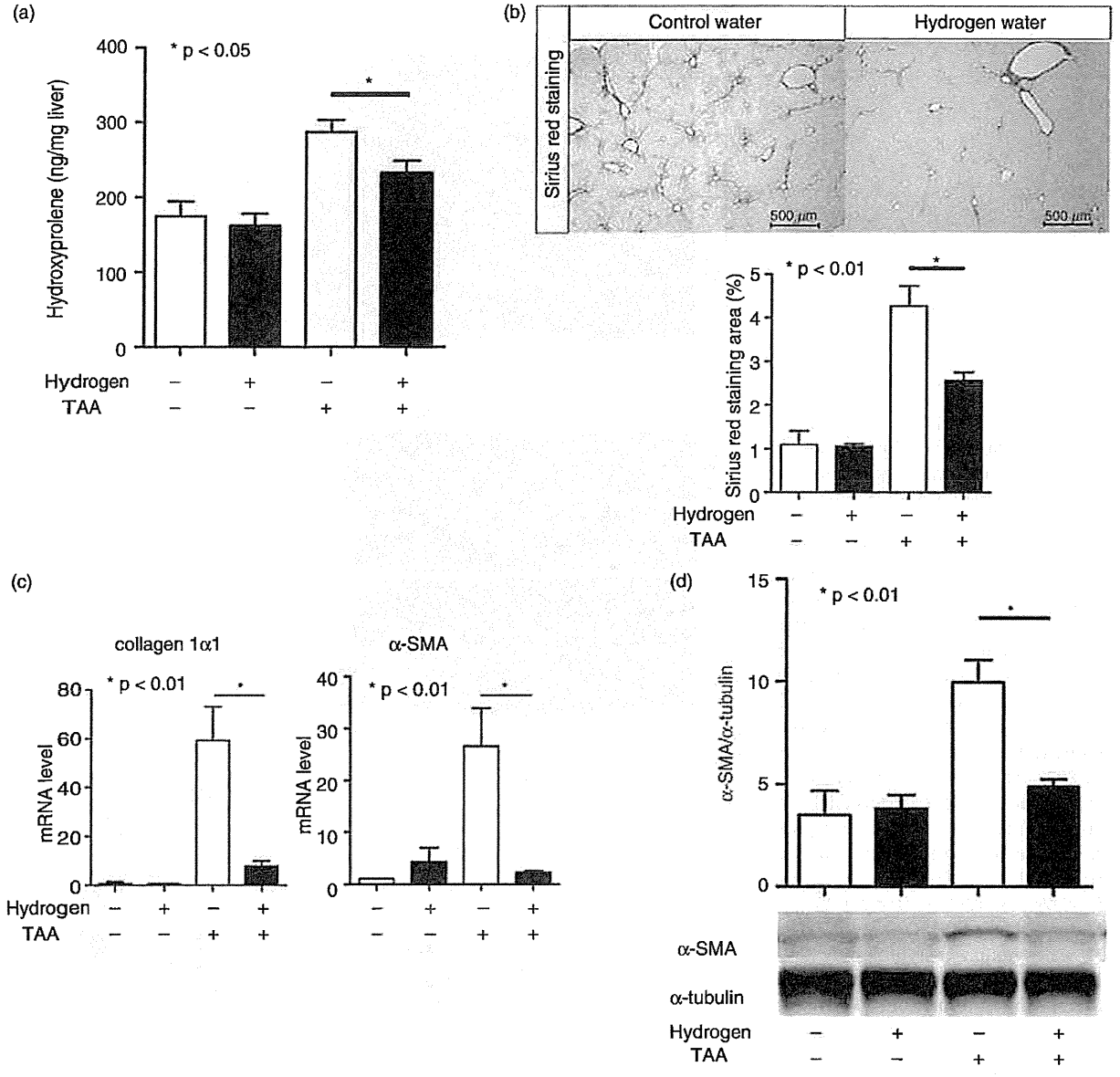

Figure 2 Oral intake of hydrogen water (H_2-water) suppresses thioacetamide (TAA)-induced liver fibrogenesis in mice. C57BL/6 mice were subjected to repeated injection with TAA and were fed with H_2-water or control water. Oral intake of H_2-water suppressed liver fibrogenesis, as assessed by hydroxyproline content (232.7 vs 287.1 ng/mg liver; $P < 0.05$) (a), Sirius red staining (b) (2.563 vs 4.271%; $P < 0.01$), reverse transcription polymerase chain reaction for collagen1α1 (7.88 vs 59.4 times that in the control; $P < 0.01$) and α-smooth muscle actin (α-SMA) (2.24 vs 26.62 times that in the control; $P < 0.01$) (c), and western blotting for α-SMA (4.86 vs 9.96 times that in the control; $P < 0.01$) (d).

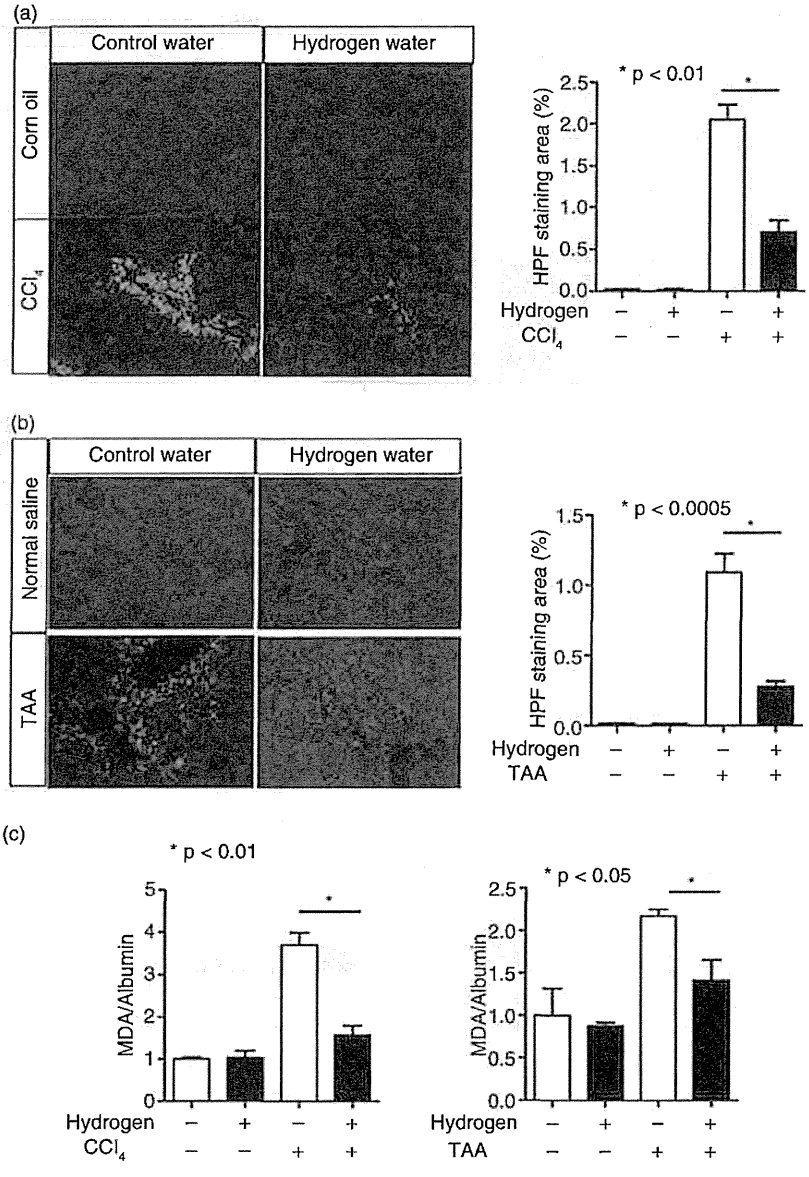

Figure 3 Oral intake of hydrogen water (H_2-water) suppresses generation of OH· in the liver. C57BL/6 mice were subjected to repeated injections of carbon tetrachloride (CCl_4) and were fed with H_2-water or control water. Generation of OH· in the liver in the CCl_4 model was assessed by hydroxyphenyl fluorescein (HPF) staining of freshly frozen liver sections. Samples from the H_2-water group had a significant smaller area of HPF staining compared to those from the control group (0.702% vs 2.051%, $P < 0.01$) (a). In the thioacetamide (TAA) model, the H_2-water group also showed a significantly smaller area of HPF staining compared to the control group (0.278% vs 1.092%, $P < 0.001$) (b). Malondialdehyde (MDA) levels in the H_2-water group were significantly lower in the CCl_4 model (3.89 vs 1.57 times that in the control) and TAA model (2.17 vs 1.41 times that in the control) (c).

Oral intake of H_2-water did not suppress liver fibrogenesis in the BDL-induced liver injury model, in which OH· was not generated

In the BDL model, no difference in hydroxyproline contents was observed between the H_2-water group and the control water group (Fig. 5a). This result was further confirmed by assessment of the mRNA expression of collagen1α1 and α-SMA (Fig. 5b) and Sirius red staining (Fig. 5c). HPF staining for the detection of OH· in freshly frozen liver sections in the BDL model showed no HPF staining in either the H_2-water or the control water groups (Fig. 5d).

Hydrogen-rich medium suppressed the generation of hydroxyl radicals and hepatocyte death induced by AMA

Antimycin A, a complex III inhibitor in the respiratory transduction system, induces the release of $O_{\cdot 2^-}$. Hepatocytes were isolated from C57BL/6 mice and treated

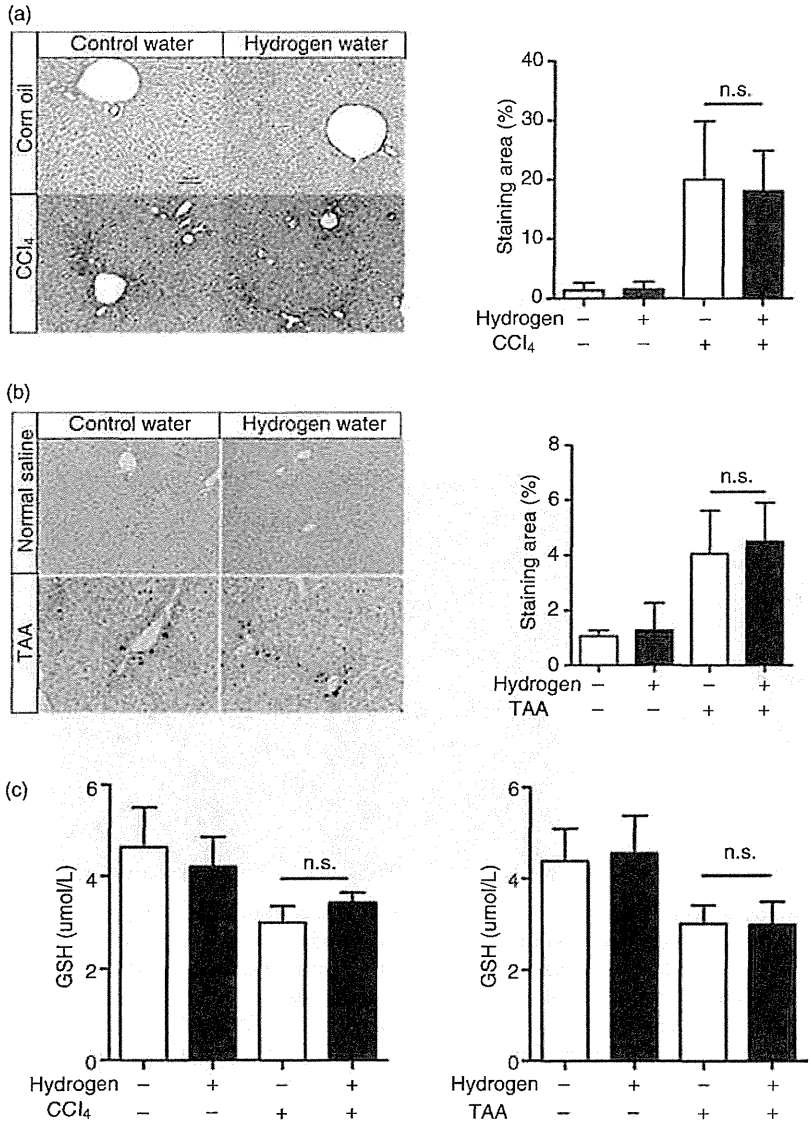

Figure 4 Oral intake of hydrogen water (H_2-water) did not affect 3-nitrotyrosine expression and glutathione (GSH). The 3-nitrotyrosine level in the liver did not differ in the carbon tetrachloride (CCl_4) model (20.1 vs 18.6 times that in the control) (a) and thioacetamide (TAA) model (4.0 vs 4.5 times that in the control) (b). GSH level in the liver did not show any difference between the control water group and the hydrogen water group both in the CCl_4 model (3.02 vs 3.44 μmol/L) and in the TAA model (3.02 vs 2.99 μmol/L) (c).

with 1 μg/mL of AMA. The addition of AMA increased levels of OH·, H_2O_2 and $O_{\cdot 2^-}$, as evaluated by the intensity of fluorescence signals emitted by the oxidized forms of HPF (Fig. 6a), CM-H_2DCFDA (Fig. 6b) and MitoSOX (Fig. 6c), respectively. Culturing in hydrogen-rich medium suppressed the generation of OH· (Fig. 6a) induced by AMA, but did not affect the increased level of H_2O_2 (Fig. 6b) or $O_{\cdot 2^-}$ (Fig. 6c), indicating that the hydrogen-rich medium selectively scavenged OH·.

Hepatocyte death induced by AMA was suppressed in the presence of hydrogen in the medium (13.2% and 26.8% for hydrogen-rich medium and control medium, respectively; $P < 0.001$) (Fig. 6d).

Hydrogen-rich medium did not suppress culture activation of HSC

We assessed the effect of culturing in hydrogen-rich medium on the activation of HSC, which are the principal fibrogenic cells in the liver. HSC are known to be activated when cultured on a plastic dish. RT–PCR for collagen1α1 and α-SMA of HSC that were cultured on a plastic dish for 5 days revealed that the hydrogen-rich medium did not suppress the activation of cultured

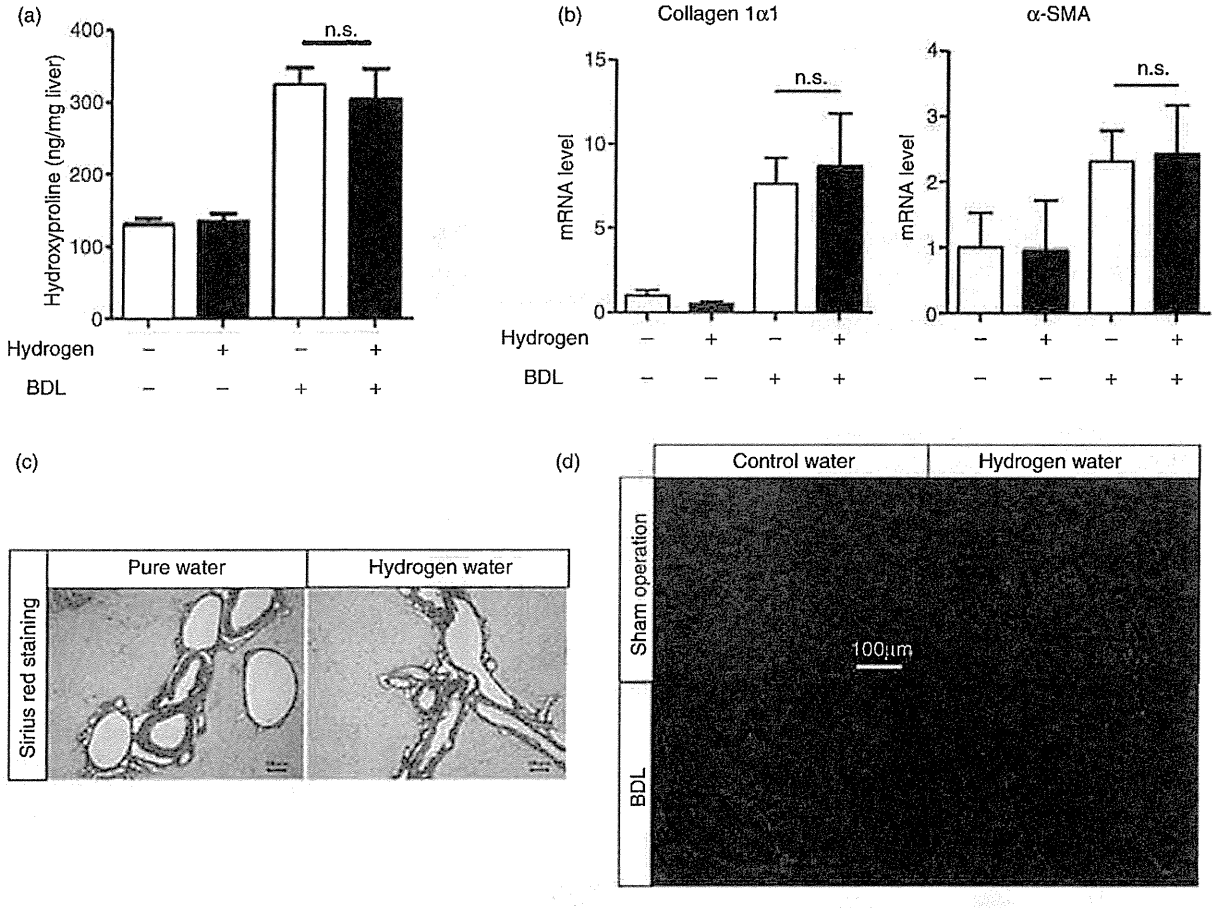

Figure 5 Oral intake of hydrogen water (H_2-water) did not suppress liver fibrogenesis in the bile duct ligation (BDL)-induced liver injury model, in which OH· was not generated. In the BDL model, hydroxyproline contents did not show any difference between the H_2-water group and the control group (a). The mRNA levels of collagen1α1 and α-smooth muscle actin (α-SMA) did not differ in the H_2-water group and the control water group (b). Sirius red staining also did not show any suppressive effect of H_2-water on liver fibrosis (c). Sirius red staining also did not show any suppressive effect of H_2-water on liver fibrosis (c). Hydroxyphenyl fluorescein staining of freshly frozen liver sections in the BDL model did not show any signs of OH· in both the H_2-water and control water groups (d).

HSC (Fig. 7a). The activated HSC showed traces of $O\cdot_{2}^{-}$, as detected by MitoSOX staining (Fig. 7b). The activated HSC contained H_2O_2, as evidenced by vivid staining with CM-H_2DCFDA (Fig. 7c), suggesting that culturing in the hydrogen-rich medium did not suppress the accumulation of H_2O_2. The HSC did not contain OH·, as evaluated by HPF staining (Fig. 7d). These results imply that OH· is not associated with the activation of cultured HSC and H_2-water does not seem to target HSC.

Hydrogen-rich medium did not suppress or accelerate HSC activation induced by AMA

Isolated HSC were cultured with or without hydrogen-rich medium in the presence of AMA to assess the effect of hydrogen on HSC activation under excess oxidative stress. Culturing in the hydrogen-rich medium did not affect the mRNA expression levels of the activation markers for HSC (collagen1α1 and α-SMA) (Fig. 8a). The increased intracellular $O\cdot_{2}^{-}$ levels induced by AMA

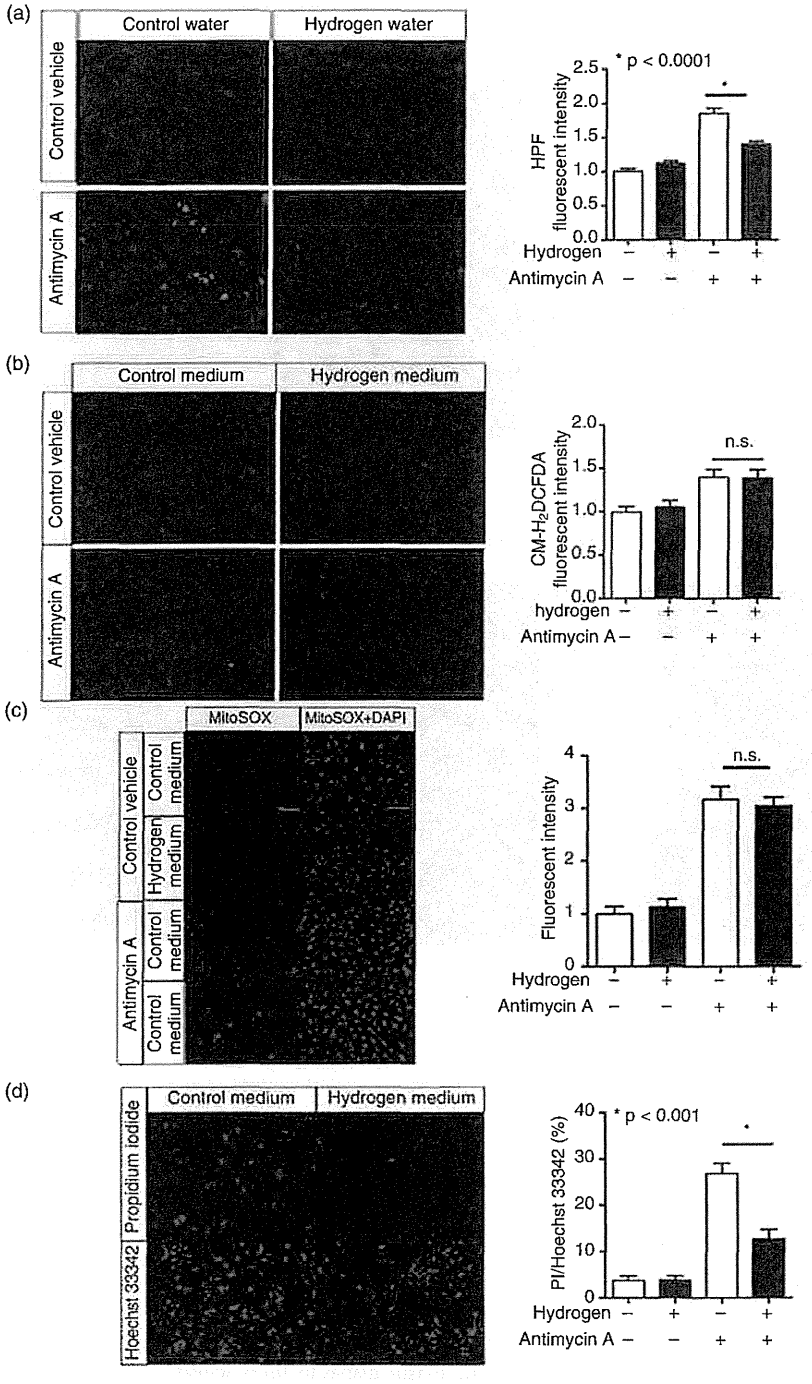

Figure 6 Hydrogen-rich medium suppresses the generation of OH· and hepatocyte death induced by antimycin A (AMA) in hepatocytes. Hepatocytes were isolated from C57BL/6 mice and treated with 1 μg/mL of AMA. Addition of AMA increased the intracellular levels of OH·, H_2O_2 and $O_{\cdot 2^-}$, as evaluated by measuring fluorescent signals emitted by the oxidized forms of hydroxyphenyl fluorescein (HPF) (a), 2′,7′-dichlorodihydrofluorescein (CM-H_2DCFDA) (b) and MitoSOX (c), respectively. Hydrogen-rich medium suppressed the generation of OH· (a), but not of H_2O_2 (d) and $O_{\cdot 2^-}$ (c). Hepatocytes were stained with Hoechst 33342 and propidium iodide (PI) and observed by fluorescent microscopy (d). AMA induced hepatocyte death. The induction of hepatocyte death was suppressed by culturing in hydrogen-rich medium (13.2% in hydrogen-rich medium vs 26.8% in control medium; $P < 0.001$) (d). DAPI, 4′,6′-diamidino-2-phenylindole dihydrochloride.

stimulation and detected by MitoSOX were not suppressed by culturing in hydrogen-rich medium (Fig. 8b). The H_2O_2 level, detected by CM-H_2DCFDA was not altered by AMA stimulation (Fig. 8c). Moreover, we could not detect intracellular OH·, even after AMA treatment (Fig. 8d). These results suggest that hydrogen did not exert its antifibrotic effect through direct action on HSC.

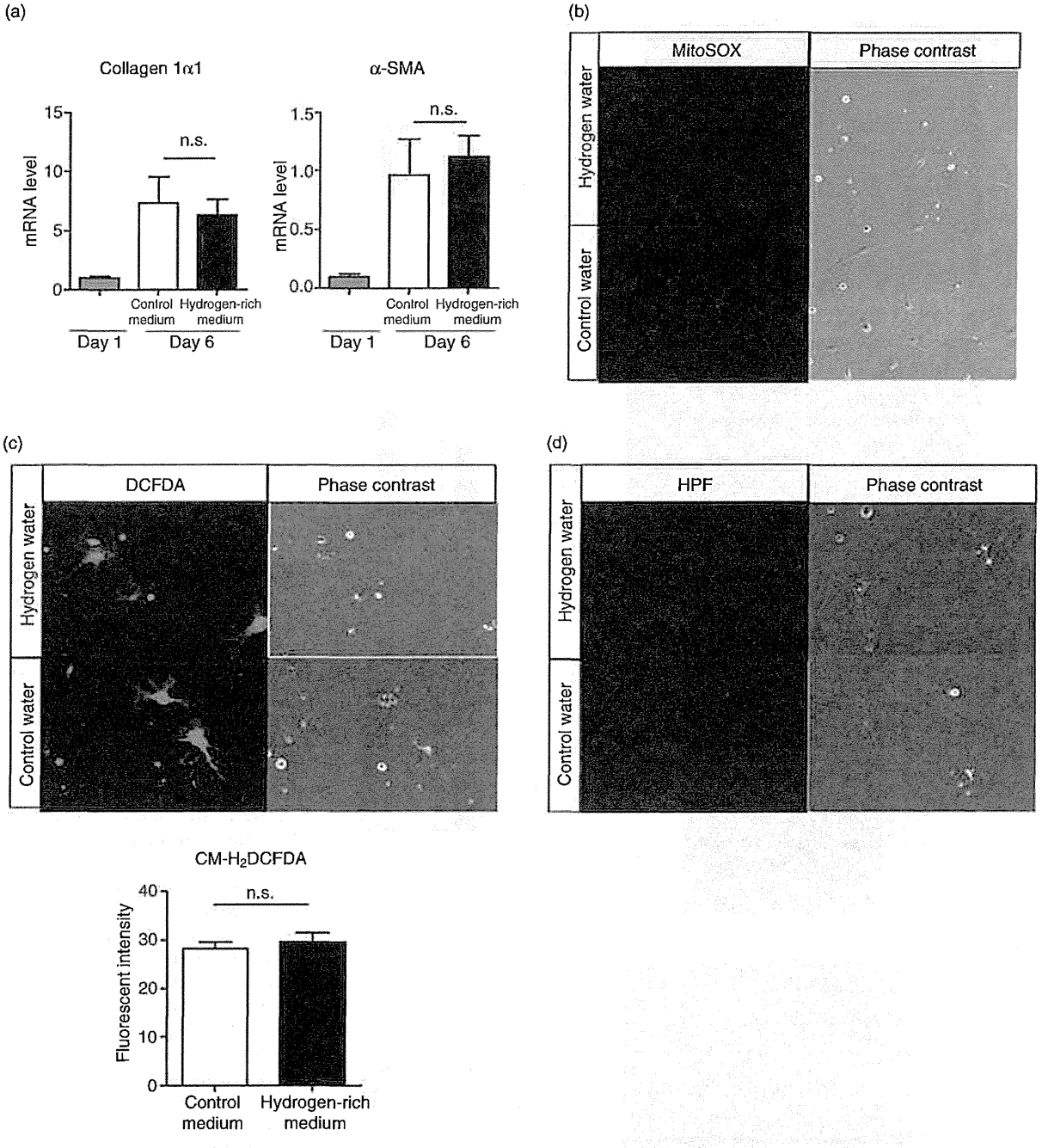

Figure 7 Hydrogen-rich medium does not suppress the activation of cultured hepatic stellate cells (HSC). HSC were isolated from C57BL/6 mice and cultured with or without hydrogen-rich medium for 5 days on plastic dishes to allow activation. Hydrogen-rich medium did not suppress the increase in the mRNA levels of HSC activation markers (collagen1α1 and α-smooth muscle actin [α-SMA]) (a). The HSC showed faint signals of $O_{\cdot 2^-}$, as detected by MitoSOX (b). HSC activated on plastic dishes showed the production of H_2O_2, as detected by 2',7'-dichlorodihydrofluorescein (CM-H_2DCFDA) (c), but culturing in hydrogen-rich medium did not show any suppressive effect on H_2O_2 production (c). The HSC did not show the presence of OH·, as detected by hydroxyphenyl fluorescein (HPF) staining (d).

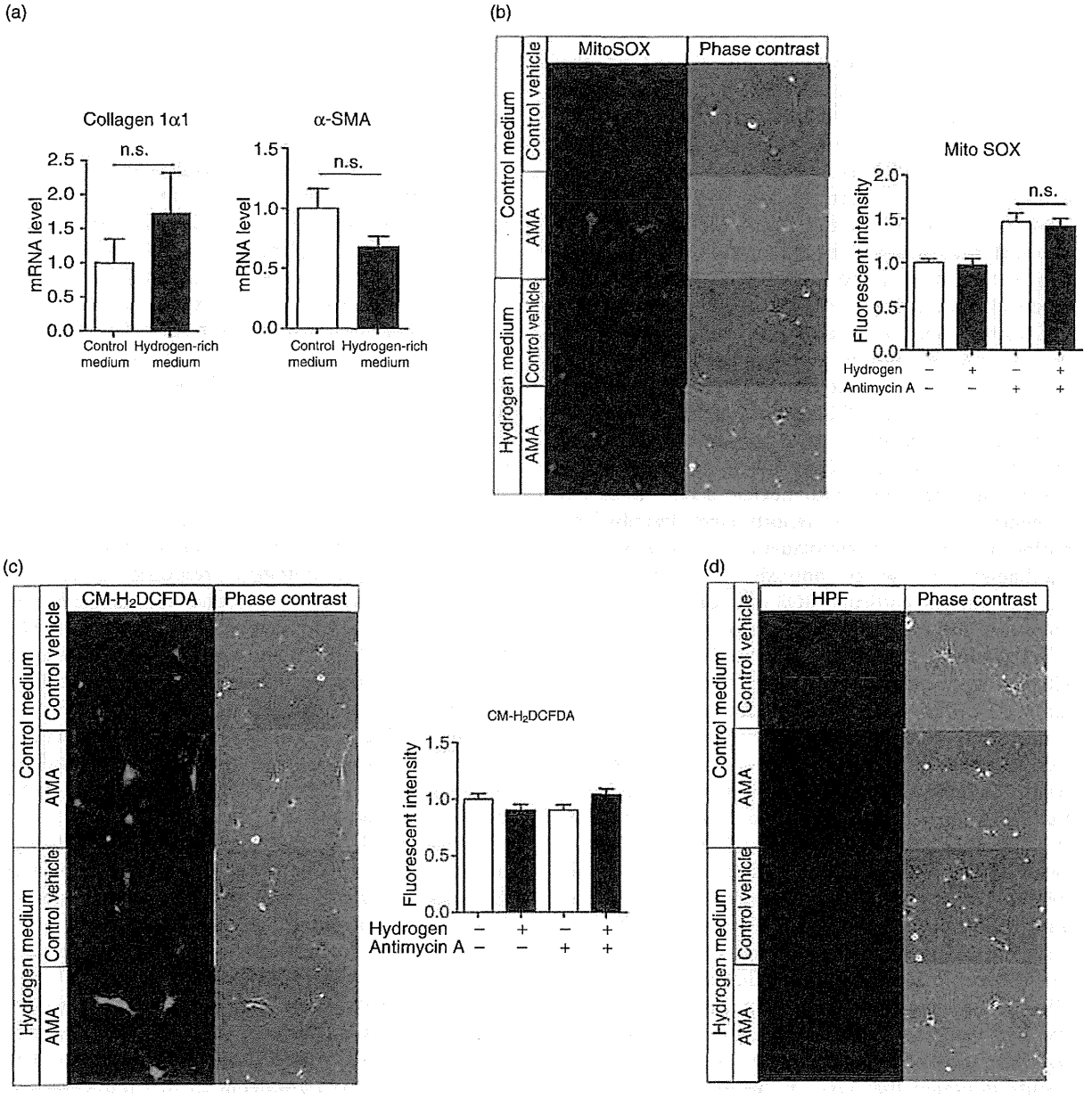

Figure 8 Hydrogen-rich medium does not suppress or accelerate the hepatic stellate cell (HSC) activation induced by antimycin A (AMA) treatment. Isolated HSC were cultured with or without hydrogen-rich medium in the presence of AMA to assess the effect of hydrogen on HSC activation under excess oxidative stress. Culturing in hydrogen-rich medium did not affect the mRNA expression levels of HSC activation markers (collagen1α1 and α-smooth muscle actin [α-SMA]) (a). Although AMA stimulation increased the intracellular level of $O_{2}^{\cdot-}$ as detected by MitoSOX (b), culturing in hydrogen-rich medium did not suppress this increase in the $O_{2}^{\cdot-}$ level. The H_2O_2 level, as detected by 2′,7′-dichlorodihydrofluorescein (CM-H_2DCFDA), was not altered by AMA stimulation (c). Moreover, we could not detect intracellular OH· even under stimulation with AMA (d).

DISCUSSION

IN THE PRESENT study, we investigated whether orally ingested H_2-water suppressed liver fibrogenesis. Our study demonstrated that H_2-water showed antifibrogenic effects in the CCl_4 and TAA models but did not show any difference in the BDL model. H_2-water exhibited an OH·-scavenging effect in the CCl_4 and TAA model; however, in the BDL model, OH· was not detected in the liver even in the control water group. We suggest that the antifibrotic effect of H_2-water is associated with the scavenging of OH·.

Carbon tetrachloride and TAA have been widely used to induce injury in experimental models of liver fibrosis. In both these models, ROS play a crucial role in the development of liver fibrosis.[22,23] Intracellular ROS usually refers to the excess amounts of $O\cdot_{2^-}$, H_2O_2 and OH·. Among them, OH· is the strongest ROS and reacts indiscriminately with nucleic acids, lipids and proteins.[10] To date, many reports have described the antifibrotic effect of antioxidants.[24–26] However, the mechanisms by which antioxidants suppress liver fibrosis, and the particular ROS that forms the primary target for antioxidants, remain to be elucidated. Galli *et al.* described the proliferation and invasiveness of HSC by $O\cdot_{2^-}$ induced by the action of xanthine and xanthine oxidase.[5] Therefore, we first sought to determine whether H_2-water exerted its antifibrotic effect through the suppression of $O\cdot_{2^-}$ production. The results of our *in vitro* experiments, however, indicated that the hydrogen-rich medium did not influence the $O\cdot_{2^-}$ and the H_2O_2 levels in both HSC and hepatocytes. We examined the expression of $O\cdot_{2^-}$ in the injured liver by staining freshly frozen liver sections with MitoSOX, and the results showed that H_2-water does not influence the $O\cdot_{2^-}$ levels in the liver (data not shown). Instead, we found that oral ingestion of H_2-water resulted in the suppression of OH· levels in the liver and that hydrogen-rich medium attenuated the generation of OH· in cultured hepatocytes. These results indicated that OH· is the primary target for H_2-water.

It is well known that peroxynitrite is a reactive oxidant produced from nitric oxide and superoxide. $O\cdot_{2^-}$ may react with nitric oxide, which could be generated constitutively from sinusoidal endothelial cell-derived nitric oxide synthase. Aram *et al.* reported that necrosis and liver fibrosis induced by CCl4 administration were decreased in inducible nitric oxide synthase deficient mice.[27] We examined 3-nitrotyrosine in the liver. Hydrogen water did not show significant effect on 3-nitrotyrosine generation in the liver. Hydrogen seems to have less effect on peroxynitrite.

With regard to the target cells of ROS in the liver, many studies have implicated oxidative stress in the activation and proliferation of HSC and hence in the development of liver fibrosis.[28,29] However, other studies have shown conflicting data as to the effects of ROS on HSC proliferation and viability.[6] Our study did not show any signs of OH· production when HSC are activated by culturing on plastic dishes. This result indicates hydrogen does not influence HSC activation directly.

On the other hand, H_2-water suppressed hepatocyte death, as demonstrated by inhibition of transaminase release in the H_2-water group. Hepatocyte injuries stimulate the phagocytosis of dead hepatocytes by Kupffer cells.[30] Activated Kupffer cells secrete profibrogenic cytokines such as TGF-β-1, which activate HSC and eventually lead to liver fibrogenesis.[31] Our *in vivo* study showed the decreased expression of TGF-β1 mRNA. Decreased induction of TGF-β1, a particularly potent profibrogenic cytokine, may be a key factor in alleviation of the fibrogenic response by H_2-water. Expression of α-SMA, an indicator for HSC activation, was also inhibited by intake of H_2-water, suggesting that inhibition of TGF-β1 induction results in reduced activation of HSC, which leads to reduced collagen deposition. Taken together, we presume that H_2-water suppresses triggering profibrogenic response by scavenging hydroxyl radicals that induce hepatocyte death and subsequent activation of Kupffer cells, TGF-β1 induction and HSC activation.

We did not detect any suppressive effect of H_2-water on fibrogenesis in BDL model. This differential effect of H_2-water on liver fibrosis caused by varying causes is interesting. This difference may be explained by the variation in the initial step triggering the inflammatory response in the two models: hepatocyte injury triggers the fibrotic pathway in hepatotoxin models, whereas biliary epithelial cell injury is the primary step triggering fibrosis in the BDL model. Therefore, the absence of the antifibrotic effect of H_2-water in the BDL model seems to be concordant with the hepatoprotective properties of H_2-water. Moreover, considering our results that indicate H_2-water selectively scavenges OH·, the difference can be explained by the variation of ROS contribution in the models: hepatocyte injuries by CCl_4 and TAA are OH·-dependent injuries, whereas biliary injury by BDL is independent of OH·.

Recent studies have demonstrated that H_2 reduces OH· and may have potential for widespread medical application as a novel, safe and effective antioxidant

with minimal adverse effects.[32] Elimination of OH· is biologically important because although $O_{\cdot 2}^{-}$ and H_2O_2 are detoxified by the antioxidant defense enzymes superoxide dismutase and peroxidase or glutathione peroxidase, no enzyme detoxifies OH·.[11]

The systemic distribution of H_2 after oral intake of H_2-water has been described previously by Kamimura *et al.*[33] They monitored the dynamic movement of hydrogen in rat liver after p.o. administration of H_2-water by introducing a needle-type hydrogen sensor into the liver. They showed that oral intake of H_2-water helps maintain a sufficient hydrogen concentration in the liver for 1 h. Further, H_2-water has already been applied in humans. Clinical trials have revealed that supplementation with H_2-water reduced oxidative stress in patients with type 2 diabetes[34] and those with potential metabolic syndrome,[35] thereby indicating that it influenced glucose[34] and cholesterol metabolism.[35] These findings indicate that H_2-water can be administrated safely to humans and has potential for use as an antifibrotic agent.

In conclusion, H_2-water protects hepatocytes from injury by scavenging OH· and thereby suppresses liver fibrogenesis in mice.

ACKNOWLEDGMENTS

THIS STUDY WAS supported by Grants-in-Aid for Scientific Research (no. 23659647, 23390322 and 21791248) from Japan Society for the Promotion of Science (JSPS). We thank Dr Akiko Taura and Dr Rie Horie for technical assistance and for providing the protocol to dissolve hydrogen into cell culture medium.

REFERENCES

1 Albanis E, Friedman SL. Hepatic fibrosis. Pathogenesis and principles of therapy. *Clin Liver Dis* 2001; 5: 315–34.
2 Bataller R, Brenner DA. Hepatic stellate cells as a target for the treatment of liver fibrosis. *Semin Liver Dis* 2001; 21: 437–51.
3 Dooley S, ten Dijke P. TGF-beta in progression of liver disease. *Cell Tissue Res* 2012; 347: 245–56.
4 Parola M, Robino G. Oxidative stress-related molecules and liver fibrosis. *J Hepatol* 2001; 35: 297–306.
5 Galli A, Svegliati-Baroni G, Ceni E *et al.* Oxidative stress stimulates proliferation and invasiveness of hepatic stellate cells via a MMP2-mediated mechanism. *Hepatology* 2005; 41: 1074–84.
6 Dunning S, Hannivoort RA, de Boer JF, Buist-Homan M, Faber KN, Moshage H. Superoxide anions and hydrogen peroxide inhibit proliferation of activated rat stellate cells and induce different modes of cell death. *Liver Int* 2009; 29: 922–32.
7 Chinopoulos C, Adam-Vizi V. Calcium, mitochondria and oxidative stress in neuronal pathology. Novel aspects of an enduring theme. *FEBS J* 2006; 273: 433–50.
8 Turrens JF. Mitochondrial formation of reactive oxygen species. *J Physiol* 2003; 552: 335–44.
9 Sauer H, Wartenberg M, Hescheler J. Reactive oxygen species as intracellular messengers during cell growth and differentiation. *Cell Physiol Biochem* 2001; 11: 173–86.
10 Halliwell B. Oxidants and human disease: some new concepts. *FASEB J* 1987; 1: 358–64.
11 Ohsawa I, Ishikawa M, Takahashi K *et al.* Hydrogen acts as a therapeutic antioxidant by selectively reducing cytotoxic oxygen radicals. *Nat Med* 2007; 13: 688–94.
12 Sun H, Chen L, Zhou W *et al.* The protective role of hydrogen-rich saline in experimental liver injury in mice. *J Hepatol* 2011; 54: 471–80.
13 Taura K, Miura K, Iwaisako K *et al.* Hepatocytes do not undergo epithelial-mesenchymal transition in liver fibrosis in mice. *Hepatology* 2010; 51: 1027–36.
14 Popov Y, Sverdlov DY, Sharma AK *et al.* Tissue transglutaminase does not affect fibrotic matrix stability or regression of liver fibrosis in mice. *Gastroenterology* 2011; 140: 1642–52.
15 Taura A, Kikkawa YS, Nakagawa T, Ito J. Hydrogen protects vestibular hair cells from free radicals. *Acta Otolaryngol Suppl* 2010; (563): 95–100.
16 Tamaki N, Hatano E, Taura K *et al.* CHOP deficiency attenuates cholestasis-induced liver fibrosis by reduction of hepatocyte injury. *Am J Physiol Gastrointest Liver Physiol* 2008; 294: G498–505.
17 Weiskirchen R, Gressner AM. Isolation and culture of hepatic stellate cells. *Methods Mol Med* 2005; 117: 99–113.
18 Iwaisako K, Hatano E, Taura K *et al.* Loss of Sept4 exacerbates liver fibrosis through the dysregulation of hepatic stellate cells. *J Hepatol* 2008; 49: 768–78.
19 Tomizawa S, Imai H, Tsukada S *et al.* The detection and quantification of highly reactive oxygen species using the novel HPF fluorescence probe in a rat model of focal cerebral ischemia. *Neurosci Res* 2005; 53: 304–13.
20 Setsukinai K, Urano Y, Kakinuma K, Majima HJ, Nagano T. Development of novel fluorescence probes that can reliably detect reactive oxygen species and distinguish specific species. *J Biol Chem* 2003; 278: 3170–5.
21 Lopez-De Leon A, Rojkind M. A simple micromethod for collagen and total protein determination in formalin-fixed paraffin-embedded sections. *J Histochem Cytochem* 1985; 33: 737–43.
22 Masuda Y. [Learning toxicology from carbon tetrachloride-induced hepatotoxicity]. *Yakugaku Zasshi* 2006; 126: 885–99.
23 Stankova P, Kucera O, Lotkova H, Rousar T, Endlicher R, Cervinkova Z. The toxic effect of thioacetamide on rat liver in vitro. *Toxicol In Vitro* 2010; 24: 2097–103.

24 Szuster-Ciesielska A, Plewka K, Daniluk J, Kandefer-Szerszen M. Betulin and betulinic acid attenuate ethanol-induced liver stellate cell activation by inhibiting reactive oxygen species (ROS), cytokine (TNF-alpha, TGF-beta) production and by influencing intracellular signaling. *Toxicology* 2011; **280**: 152–63.
25 Ohyama T, Sato K, Kishimoto K *et al.* Azelnidipine is a calcium blocker that attenuates liver fibrosis and may increase antioxidant defence. *Br J Pharmacol* 2012; **165**: 1173–87.
26 Paik YH, Yoon YJ, Lee HC *et al.* Antifibrotic effects of magnesium lithospermate B on hepatic stellate cells and thioacetamide-induced cirrhotic rats. *Exp Mol Med* 2011; **43**: 341–9.
27 Aram G, Potter JJ, Liu X, Torbenson MS, Mezey E. Lack of inducible nitric oxide synthase leads to increased hepatic apoptosis and decreased fibrosis in mice after chronic carbon tetrachloride administration. *Hepatology* 2008; **47**: 2051–8.
28 Paik YH, Iwaisako K, Seki E *et al.* The nicotinamide adenine dinucleotide phosphate oxidase (NOX) homologues NOX1 and NOX2/gp91(phox) mediate hepatic fibrosis in mice. *Hepatology* 2011; **53**: 1730–41.
29 Li J, Fan R, Zhao S *et al.* Reactive oxygen species released from hypoxic hepatocytes regulates MMP-2 expression in hepatic stellate cells. *Int J Mol Sci* 2011; **12**: 2434–47.
30 Canbay A, Feldstein AE, Higuchi H *et al.* Kupffer cell engulfment of apoptotic bodies stimulates death ligand and cytokine expression. *Hepatology* 2003; **38**: 1188–98.
31 Gressner AM, Bachem MG. Molecular mechanisms of liver fibrogenesis – a homage to the role of activated fat-storing cells. *Digestion* 1995; **56**: 335–46.
32 Terasaki Y, Ohsawa I, Terasaki M *et al.* Hydrogen therapy attenuates irradiation-induced lung damage by reducing oxidative stress. *Am J Physiol Lung Cell Mol Physiol* 2011; **301**: L415–426.
33 Kamimura N, Nishimaki K, Ohsawa I, Ohta S. Molecular hydrogen improves obesity and diabetes by inducing hepatic FGF21 and stimulating energy metabolism in db/db mice. *Obesity (Silver Spring)* 2011; **19**: 1396–403.
34 Kajiyama S, Hasegawa G, Asano M *et al.* Supplementation of hydrogen-rich water improves lipid and glucose metabolism in patients with type 2 diabetes or impaired glucose tolerance. *Nutr Res* 2008; **28**: 137–43.
35 Nakao A, Toyoda Y, Sharma P, Evans M, Guthrie N. Effectiveness of hydrogen rich water on antioxidant status of subjects with potential metabolic syndrome-an open label pilot study. *J Clin Biochem Nutr* 2010; **46**: 140–9.

Journal of Gastroenterology and Hepatology

JGHF

doi:10.1111/jgh.12376

HEPATOLOGY

Relationship between inosine triphosphate genotype and outcome of extended therapy in hepatitis C virus patients with a late viral response to pegylated-interferon and ribavirin

Hoang Hai,* Akihiro Tamori,* Masaru Enomoto,* Hiroyasu Morikawa,* Sawako Uchida-Kobayashi,* Hideki Fujii,* Atsushi Hagihara,* Etsushi Kawamura,* Le Thi Thanh Thuy,* Yasuhito Tanaka† and Norifumi Kawada*

*Department of Hepatology, Osaka City University Graduate School of Medicine, Osaka, and †Department of Virology and Liver Unit, Nagoya City University Graduate School of Medical Sciences, Nagoya, Japan

Key words
extended therapy, HCV, *ITPA* genotype, treatment outcome.

Accepted for publication 12 August 2013.

Correspondence
Dr Akihiro Tamori, Department of Hepatology, Osaka City University Graduate School of Medicine, 1-4-3, Asahi-machi, Abenoku, Osaka 545-8585, Japan. Email: atamori@med.osaka-cu.ac.jp

Conflict of interest: In the past year, Dr Akihiro Tamori has received research funding from MSD K.K. Dr Yasuhito Tanaka has consulted for MSD K.K and Chugai Pharmaceutical Co., Ltd., and has received research funding from MSD K.K and Chugai Pharmaceutical Co., Ltd. Dr Norifumi Kawada has consulted for MSD K.K and Chugai Pharmaceutical Co., Ltd., and has received research funding from MSD K.K and Chugai Pharmaceutical Co., Ltd. Other authors report no conflicts of interest.

The English in this document has been checked by at least two professional editors, both native speakers of English. For a certificate, please see http://www.textcheck.com/certificate/mXLRyV

Abstract

Background and Aim: It is not yet clear which factors are associated with the outcome of 72-week treatment with pegylated-interferon and ribavirin (RBV) in patients with chronic hepatitis C virus (HCV) infection.

Methods: In 66 patients with HCV genotype 1 who had a late viral response (LVR) to 72-week treatment of pegylated-interferon and RBV, we examined the factors that determined the outcome, including single nucleotide polymorphisms of interleukin-28B and inosine triphosphatase (*ITPA*) genes.

Results: Thirty seven of 66 (56%) patients with LVR achieved a sustained viral response (SVR). The mean age of these 37 SVR patients was 55, compared with 61 in 29 relapsed patients ($P = 0.009$). Twenty six of 54 (48%) patients with the CC genotype and 11 of 12 (92%) with the CA/AA genotype of *ITPA* rs1127354 achieved SVR ($P = 0.006$). The SVR rates were 79%, 40%, 60%, and 33% in patients with undetectable HCV RNA on weeks 16, 20, 24, and 28 or later, respectively ($P = 0.014$). Finally, serum RBV concentration at week 44 of treatment was significantly higher in the SVR group (2651 ng/mL) than in the relapse group (1989 ng/mL, $P = 0.002$). In contrast, the rate of the interleukin-28B genotype was not different between the groups. Multiple regression analysis showed that age < 60 years, *ITPA* CA/AA genotype, and serum RBV concentration were significant independent predictive factors for SVR.

Conclusions: Our findings elucidated the association of four factors, including *ITPA* genotype, with the outcome of 72-week treatment in LVR patients.

Introduction

Hepatitis C virus (HCV) infection continues to be a major cause of liver cirrhosis and hepatocellular carcinoma.[1] An estimated 120–130 million people worldwide are infected with HCV.[2] Sustained viral response (SVR), defined as undetectable serum HCV RNA levels 24 weeks after cessation of therapy, is the aim of treatment. Although the current treatment regimen of pegylated-interferon (PEG-IFN) combined with ribavirin (RBV) greatly improved SVR in patients with HCV genotypes 2 and 3, the outcomes in patients with HCV genotype 1 and high viral load (> 10^5 IU/mL) remain unsatisfactory, and SVR is attained in approximately 50% of cases.[3–8]

For HCV genotype 1, patients with rapid viral response, defined as undetectable serum HCV on week 4, achieve high rates of SVR up to 91% with combination therapy. Patients with early viral

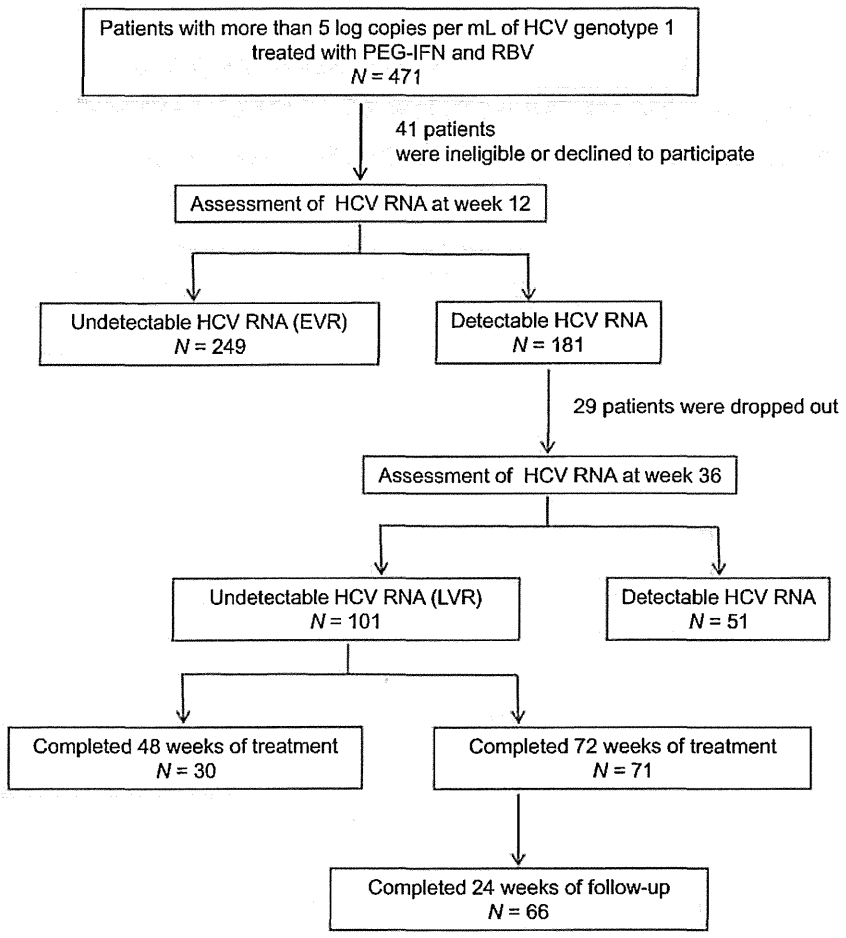

Figure 1 Flow of participants throughout the study. EVR, early viral response; HCV, hepatitis C virus; LVR, late viral response; PEG-IFN, pegylated-interferon; RBV, ribavirin.

response, defined as undetectable serum HCV on week 12, achieved SVR rates of 65–81%. However, patients with a late viral response (LVR), who remained positive for HCV RNA on week 12 after the start of treatment but became negative for HCV RNA during weeks 13–36 of treatment, showed a lower SVR rate of 14–44%.[4,9–19] Although extending therapy to 72 weeks has been reported to decrease relapse in such patients,[12–17,20,21] it remains unclear which patient with LVR can benefit from extended treatment.

Inosine triphosphatase (*ITPA*) single nucleotide polymorphism (SNP) rs1127354, causing ITPase deficiency, was found to be associated with protection from RBV-induced anemia and to decrease the need for RBV dose reduction, but not to be associated with clinical outcome.[22–25] The present study was performed to identify that factors, including interleukin-28B (*IL28B*) and *ITPA* genotype, associated with the outcome of extended 72-week treatment in patients with HCV genotype 1 who had LVR to PEG-IFN and RBV.

Methods

Patients. A total of 471 patients were recruited at Osaka City University Hospital between December 2004 and June 2012. The flow of patients through the trial is presented in Figure 1. Sixty-six patients with HCV genotype 1 who were treated with PEG-IFN alpha 2a (Pegasys; Chugai Pharmaceutical Co., Ltd, Tokyo, Japan) or 2b (Pegintron; MSD, Osaka, Japan) and RBV (Rebetol, MSD) combination therapy were enrolled in this study. All patients had a viral load of $> 10^5$ IU/mL according to COBAS Amplicor HCV Monitor test, version 2.0 (Roche Diagnostics, Branchburg, NJ, USA), or a viral load of > 5 log copies/mL as determined by COBAS TaqMan HCV test (Roche Diagnostics). HCV RNA levels were investigated before and every 4 weeks after the start of treatment. All patients gave written informed consent to participate in this study, in accordance with the ethical guidelines of the 1975 Declaration of Helsinki and according to the process approved by the ethical committee of Osaka City University, Graduate School of Medicine. Only the patients who completed 72-week combination therapy without discontinuation and in whom HCV RNA was detected on week 12 but not on weeks 13–36 were enrolled in this study.

Exclusion criteria included a history or evidence of a serious chronic or poorly controlled medical or psychiatric condition, infection with human immunodeficiency virus or hepatitis B virus, and receipt of systemic immunomodulatory or antineoplastic therapy within the previous 6 months. Pregnant or breastfeeding women and partners of pregnant women were also excluded.

The following factors were analyzed to determine whether they were related to the efficacy of combination therapy: patient age, gender, pretreatment biochemical parameters, such as neutrophil and platelet counts, hemoglobin concentration, levels of alanine transaminase, creatinine, HCV viral load, histopathological evaluation of hepatitis activity and hepatic fibrosis according to the METAVIR scoring system, total doses of PEG-IFN and RBV, and serum RBV concentration at week 44.

Treatment protocol. The initial dose of PEG-IFN alpha 2a was 180 μg per week, and that of PEG-IFN alpha 2b was 1.5 μg per kg body weight per week. The initial dose of RBV was 400, 600, 800, or 1000 mg/day for patients weighing < 40 kg, 40–60 kg, 60–80 kg, or > 80 kg, respectively.

RBV concentration. Serum RBV concentration was measured using an assay consisting of phenylboronic acid solid phase extraction, followed by HPLC at a commercial laboratory (SRL Inc., Osaka, Japan).[26] Briefly, the RBV concentrations in 200-μL samples were measured by validated HPLC with column switching. Serum samples deproteinized with perchloric acid were injected into the column, and RBV was detected by monitoring absorption of ultraviolet at 215 nm. The calibration curve was linear in the range of 50–20 000 ng/mL. A set of calibration standards at 0, 5, 10, 25, 50, 100, 250, 500, 1000, 2000, and 5000 mg/L RBV was prepared, extracted and analyzed with each series, together with internal quality controls at three levels.

SNP genotyping. We examined genetic polymorphisms of the *IL28B* and *ITPA* genes in patients who consented to genome analysis. Whole blood was collected from all patients and centrifuged to separate the buffy coat. Genomic DNA was extracted from the buffy coat using a QIAamp DNA Blood Midi Kit (Qiagen Sciences Inc, Germantown, MD, USA). Genetic polymorphisms of *IL28B* rs8099917 and rs12979860 and *ITPA* rs1127354 were genotyped by TaqMan SNP Genotyping Assay on the 7500 Fast Real-Time PCR System (Applied Biosystems, Foster City, CA, USA). All samples were also genotyped by direct sequencing to confirm the genotype. Exon 2 of the *ITPA* gene and flanking intronic regions were amplified by polymerase chain reaction (PCR) using the following primers: forward, 5′-CTTTAGG AGATGGGCAGCAG-3′; reverse, 5′-CACAGAAAGTCAGGTC ACAGG-3′.[27] PCR was carried out in a total volume of 15 μL with 1× Premix Ex Tag (Applied Biosystems), 300 nM of each primer, and 100 ng of genomic DNA. The PCR profile consisted of 94°C for 10 min, followed by 35 cycles of 94°C for 30 s, 63°C for 30 s, and 72°C for 1 min, with a final extension at 72°C for 7 min. PCR products were sequenced bidirectionally using a BigDye Terminator v3.1 Cycle Sequencing Kit and ABI 3130XL Genetic Analyzer (Applied Biosystems). Genotyping analysis was permitted by the ethical committee of our university (approval number 1871).

Statistical analysis. All data analyses were conducted using the JMP program, version 9.0 (SAS Institute, Cary, NC, USA). Individual characteristics between groups were evaluated by Wilcoxon's two-sample test for numerical variables, or Fisher's exact test for categorical variables. Variables exhibiting values of $P < 0.1$ on univariate analysis were subjected to stepwise multivariate logistic regression analysis. In the two-tailed test, $P < 0.05$ was taken to indicate statistical significance.

Table 1 Characteristics of HCV genotype 1 patients with late virologic response†

	Total (n = 66)
Age (years)	60 (21–77)
Gender (male/female)	43/23
HCV viral load (log copies/mL)	6.5 (5.1–7.7)
Body mass index (kg/m^2)	22.7 (16.5–28.0)
WBC (/μL)	4600 (2000–8600)
Hb (g/dL)	13.6 (10.9–17.3)
Platelet (× 10^4/μL)	17.1 (8.5–45.0)
ALT (IU/L)	54 (17–194)
Creatinine (mg/dL)	0.66 (0.36–1.16)
IL28B rs8099917 (TT/TG+GG)	45/21
IL28B rs12979860 (CC/CT+TT)	44/22
ITPA rs1127354 (CC/CA+AA)	54/12
Liver biopsy	
Activity grading (0/1/2/3/ND)	7/40/13/1/5
Fibrosis staging (1/2/3/4/ND)	38/15/8/0/5
PEG-IFNα2a/PEG-IFNα2b	12/54
Week when HCV RNA was undetectable (16 weeks/20 weeks/24 weeks/28 weeks or delayed)	24/20/10/12
RBV concentration at week 44 (ng/mL)	2467 (1006–4283)
Total dose of administered RBV (g/kg body weight)	5.07 (1.56–7.21)

†Continuous variables are medians (min-max).
ALT, alanine transaminase; Hb, hemoglobin; HCV, hepatitis C virus; *IL28B*, interleukin 28B gene; *ITPA*, inosine triphosphatase gene; ND, not done; PEG-IFN, pegylated-interferon; RBV, ribavirin; WBC, white blood cell.

Results

Patient profile and response rate. The characteristics of the overall 66 LVR patients, consisting of 43 men and 23 women, are shown in Table 1. The mean age of this cohort was 60 years. All of the patients who were infected with HCV genotype 1 with viral load > 5 log copies/mL, were treated with PEG-IFN/RBV for 72 weeks. HCV RNA was tested 24 weeks after completion of treatment when SVR and relapse were defined if HCV RNA was negative and positive, respectively. After 72 weeks of combination therapy, 37 (56%) patients achieved SVR, while the remaining 29 (44%) relapsed.

Direct sequencing and TaqMan SNP genotyping assay were used to genotype SNP *ITPA* rs1127354, and 100% of SNP results were concordant between both methods. Among the 66 LVR patients, 54 (82%) had the major CC genotype (wild-type), 10 (15%) were heterozygous for the CA genotype, and the remaining 2 (3%) had the minor AA genotype.

Association between clinical factors and SVR rate. Among the 17 factors screened by univariate analysis, four factors were associated with treatment response, that is, patient

Table 2 Comparison of the clinical characteristics of patients with SVR and those with relapse†

	SVR (n = 37)	Relapse (n = 29)	P-value
Age (years)	55 ± 7	61 ± 7	0.009*
Gender (male/female)	24/13	19/10	0.956
HCV viral load (log copies/mL)	6.6 ± 0.4	6.4 ± 0.5	0.195
Body mass index (kg/m^2)	22.6 ± 2.9	22.1 ± 2.5	0.438
WBC (/μL)	4748 ± 1235	4693 ± 1281	0.861
Hb (g/dL)	13.9 ± 1.3	13.9 ± 1.6	0.892
Platelets (× 10^4/μL)	18.2 ± 7.8	16.6 ± 4	0.698
ALT (IU/L)	63.8 ± 40.6	62.6 ± 37.9	0.861
Creatinine (mg/dL)	0.71 ± 0.19	0.67 ± 0.12	0.473
IL28B rs8099917 (TT/TG+GG)	25/12	20/9	0.904
IL28B rs12979860 (CC/CT+TT)	24/13	20/9	0.930
ITPA rs1127354 (CC/CA+AA)	26/11	28/1	0.006*
Liver biopsy			
Activity grading (0/1/2/3/ND)	3/24/6/1/3	4/16/7/0/2	0.563
Fibrosis staging (1/2/3/4/ND)	20/11/3/0/3	18/4/5/0/2	0.211
PEG-IFNα2a/PEG-IFNα2b	6/31	6/23	0.64
Week when HCV RNA was undetectable (16 weeks/20 weeks/24 weeks/28 weeks or delayed)	19/8/6/4	5/12/4/8	0.014*
RBV concentration at week 44 (ng/mL)	2651 ± 675	1989 ± 525	0.002*
Total dose of RBV administered (g/kg body weight)	5.08 ± 1.3	4.59 ± 1.11	0.059

*P < 0.05.
†Continuous variables are medians (min-max).
ALT, alanine transaminase; Hb, hemoglobin; HCV, hepatitis C virus; *IL28B*, interleukin 28B gene; *ITPA*, inosine triphosphatase gene; ND, not done; PEG-IFN, pegylated interferon; RBV, ribavirin; WBC, white blood cell.

age, *ITPA* SNP rs1127354, time of undetectable HCV RNA, and RBV concentration (Table 2). The mean age of patients with SVR was significantly younger than that of patients with relapse (55 *vs* 61 years, respectively, $P = 0.009$). Eleven of 37 (30%) patients with SVR and 1 of 29 (3%) patients with relapse had the CA/AA genotype of *ITPA*, indicating a significant association between the CA/AA genotype and SVR ($P = 0.006$). In contrast, the proportion of the *IL28B* genotype was not different between patients with SVR and relapse. Earlier HCV RNA disappearance was significantly associated with treatment outcome ($P = 0.014$); SVR rate was 79% (19/24) in patients with undetectable HCV RNA on week 16, 40% (8/20) on week 20, 60% (6/10) on week 24, and 33% (4/12) on or after week 28 (Fig. 2). Finally, when RBV concentration in the peripheral blood was examined on week 44 of treatment, it was significantly higher in the SVR group (2651 ng/mL) than the relapse group (1989 ng/mL, $P = 0.002$).

Association between SNP ITPA rs1127354 and clinical factors. Twenty six of 54 (48%) patients with the CC genotype and 11 of 12 (92%) with the CA/AA genotype achieved SVR (Fig. 3), indicating a significant association between the CA/AA genotype and SVR ($P = 0.006$). The decline in hemoglobin concentration on week 12 from the baseline was 3.56 g/dL in patients with the CC genotype, compared with 2.16 g/dL in CA/AA patients ($P = 0.0004$, Fig. 4a).

Evaluation of the association between SNP rs1127354 and RBV concentration or total dose of administered RBV showed no significance ($P = 0.27$ and 0.65, respectively) (Fig. 4b,c).

Independent predictive factors of combination therapy for SVR. Factors exhibiting values of $P < 0.1$ on univariate analysis were age, *ITPA* genotype, week at which HCV

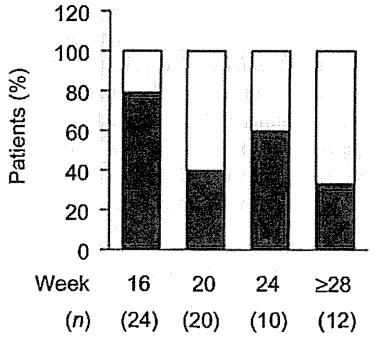

Figure 2 Effects of combination therapy in patients with genotype 1 according to the time at which HCV was undetectable (week). Earlier HCV RNA disappearance was significantly associated with treatment outcome ($P = 0.014$). SVR rates were 79% (19/24) in patients with undetectable HCV RNA at week 16, 40% (8/20) at week 20, 60% (6/10) at week 24, and 33% (4/12) at week 28 or delayed. HCV, hepatitis C virus; SVR, sustained viral response. (□) Relapse, (■) SVR.

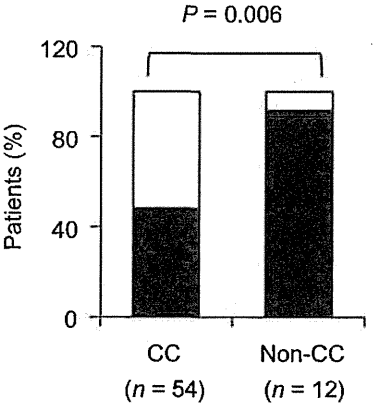

Figure 3 Effects of combination therapy in patients with genotype 1 according to *ITPA* SNP rs1127354 genotype. SVR (black bar) was achieved in 48% (26/54) of patients with the rs1127354 CC genotype, and in 92% (11/12) of those with a non-CC genotype at rs1127354. Patients with the rs1127354 CA/AA genotype were significantly more likely to be associated with SVR ($P = 0.006$). In the relapse group (white bar), the major CC allele occurred in 28/54 patients but the minor CC allele in only 1/12 patients. *ITPA*, inosine triphosphatase gene; SNP, single nucleotide polymorphism; SVR, sustained viral response. (□) Relapse, (■) SVR.